In vivo engineering of organs: The bone bioreactor

Molly M. Stevens*†, Robert P. Marini‡, Dirk Schaefer§¶, Joshua Aronson*, Robert Langer*, and V. Prasad Shastri‖**

*Department of Chemical Engineering, Massachusetts Institute of Technology, 45 Carleton Street, E25-342, Cambridge, MA 02139; †Department of Materials, Imperial College London, Prince Consort Road, London SW7 2AZ, United Kingdom; ‡Division of Comparative Medicine, Massachusetts Institute of Technology, 45 Carleton Street, E25-021, Cambridge, MA 02139; ¶Department of Surgery, University of Basel, Spitalstrasse 21, 4031 Basel, Switzerland; and ‖Department of Biomedical Engineering, Vanderbilt University, 5824 Stevenson Center, Nashville, TN 37232

Contributed by Robert Langer, June 8, 2005

Treatment of large defects requires the harvest of fresh living bone from the iliac crest. Harvest of this limited supply of bone is accompanied by extreme pain and morbidity. This has prompted the exploration of other alternatives to generate new bone using traditional principles of tissue engineering, wherein harvested cells are combined with porous scaffolds and stimulated with exogenous mitogens and morphogens *in vitro* and/or *in vivo*. We now show that large volumes of bone can be engineered in a predictable manner, without the need for cell transplantation and growth factor administration. The crux of the approach lies in the deliberate creation and manipulation of an artificial space (bioreactor) between the tibia and the periosteum, a mesenchymal layer rich in pluripotent cells, in such a way that the body's healing mechanism is leveraged in the engineering of neotissue. Using the "*in vivo* bioreactor" in New Zealand White rabbits, we have engineered bone that is biomechanically identical to native bone. The neobone formation followed predominantly an intramembraneous path, with woven bone matrix subsequently maturing into fully mineralized compact bone exhibiting all of the histological markers and mechanical properties of native bone. We harvested the bone after 6 weeks and transplanted it into contralateral tibial defects, resulting in complete integration after 6 weeks with no apparent morbidity at the donor site. Furthermore, in a proof-of-principle study, we have shown that by inhibiting angiogenesis and promoting a more hypoxic environment within the "*in vivo* bioreactor space," cartilage formation can be exclusively promoted.

cartilage | tissue engineering | hard tissue | vascularized organs

Bone is a highly vascularized tissue, with an intricate cellular architecture that continues to remodel throughout the lifetime of an individual. Despite the regenerative capacity of bone, large bone defects, as observed after bone tumor resections and severe fractures, lack the template for an orchestrated regeneration and require bone grafting (1). Furthermore, annually >200,000 spinal fusions are performed in the U.S. alone that also require massive bone grafting (2). In spinal fusion and long-bone fractures, autologous bone is considered the gold standard because of its ability to integrate with the host bone and its lack of immune-related complications (3). Nevertheless, the use of autologous bone has been hampered by its short supply and the pain and long-term discomfort that accompany such harvests from the iliac crest (4). Hence, increasing the autologous source of bone while addressing harvest-related morbidity issues would have a significant impact on the field of orthopedics, and this has prompted the exploration of other alternatives (4).

Despite numerous attempts, *in vitro* engineering of functional bone tissue using principles of tissue engineering has proven elusive because of the challenges involved in the differentiation and sustenance of different cell types in a concomitant fashion and in achieving a vascular network *in vitro*. Recently, *in vivo* engineering of bone has been demonstrated by combining porous ceramic or demineralized bone matrix supports with mesenchymal (marrow-derived) cells and/or bone morphogenetic proteins (5–10). The administration of exogenous growth factors and cell isolation and transplantation have generally been considered essential prerequisites to tissue-engineering approaches (11). We now demonstrate an approach for the *in vivo* engineering of large predictable volumes of autologous bone without the need for harvest/expansion of cells and use of growth factors.

Our approach is based on the manipulation of a deliberately created space within the body, such that it serves as an "*in vivo* bioreactor," wherein the engineering of the neotissue is achieved by invocation of a healing response within the bioreactor space. Specifically, in the context of bone engineering, we hypothesized that by creating this "space" between the surface of a long bone and the membrane rich in pluripotent cells that covers it, namely the periosteum, the cell population and biomolecular signals necessary for the formation of bone could be locally derived. We created such bioreactors in the tibia of New Zealand White rabbits and then provided volume to this space by injecting a biocompatible calcium-alginate gel that crosslinked *in situ*, and we followed their maturation over 12 weeks. We observed that, as hypothesized, the bioreactor space was reconstituted by functional living bone. Furthermore, the engineered bone was easily harvested without any apparent postoperative morbidity to the subject and transplanted successfully in a contralateral defect.

Methods

Preparation of Alginate Gel. The 1% (wt/vol) alginate gel used in these studies was optimized from a series of 70 gels developed and characterized as reported in detail elsewhere (12, 13). Briefly, gelation was triggered by mixing a 2% (wt/vol) sodium alginate (FMC BioPolymer) in 30 mM Hepes containing 150 mM NaCl and 10 mM KCl, with an equal volume of a solution containing 75 mM $CaCl_2$ in 10 mM Hepes containing 150 mM NaCl and 10 mM KCl by using a sterile Y-piece mixer. The gel cured within 1 min and had a Young's modulus of 0.17 MPa. Growth factors (TGF-β1 and FGF-2, R & D Systems) were included in the formulation at a concentration of 10 ng/ml where indicated. The growth factor combination and their concentrations in the gel were based on our earlier findings that they enhanced cell proliferation and differentiation in periosteal explants organ cultures *in vitro* (13).

Preparation of Hyaluronic Acid (HA)-Based Gel. The HA-based gel used in these studies was prepared by using a previously reported strategy (14). Briefly, HA (Genzyme) was chemically modified to bear aldehyde groups (HA-ALD) by reaction with sodium periodate and hydrazide groups (HA-ADH) by reacting with adipic dihydrazide. HA hydrogels were produced by mixing equal volumes of 2% (wt/vol) aqueous solutions of HA-ALD and HA-ADH. Suramin (Bayer, Leverkusen, Germany) was included in free (0.4 mol/liter) and liposome-encapsulated (0.4 mol/liter) forms where indicated during the gelation. Suramin-

Abbreviations: HA, hyaluronic acid; H&E, hematoxylin/eosin.

§Deceased October 8, 2004.

**To whom correspondence should be addressed. E-mail: prasad.shastri@vanderbilt.edu.

www.pnas.org/cgi/doi/10.1073/pnas.0504705102

containing liposomes were prepared by using a previously reported method (15, 16).

Animal Surgeries. ***Creation of the bone bioreactor.*** The study involved 26 skeletally mature New Zealand White rabbits. The muscle on the anteromedial aspect of the metaphyseal and diaphyseal tibia was incised and retracted caudad to expose the periosteum. A 5/8-in 25-gauge needle was bent at a 45° angle halfway along its length and was attached to a 3-ml syringe filled with Ringer's solution. The periosteum was pierced by the needle, bevel up, and separated from the bone by simultaneous infusion of fluid between the cambium and the bone and slow advancement of the needle in a lateral sweeping motion (17). When a subperiosteal space of adequate size had been created, gel was injected through the pinhole-sized entry point into the space until full distension (bioreactor dimensions 3 cm long, 0.7 cm wide, and 1 mm above the plane of the tibia; volume $\approx$ 200 mm^3) was achieved. The hole in the periosteum was sealed by fibrin glue (Baxter Healthcare, Mundelein, IL) and the incision closed with sutures. After death, legs were harvested by amputation at the femorotibial joint.

Transplantation of autologous neoosseous tissue harvested from the bone bioreactor. Neoosseous tissue was harvested with an osteotome from the right tibia of four rabbits 6 weeks after bioreactor creation. A 7 $\times$ 3 $\times$ 1.5-mm (length $\times$ width $\times$ depth) cortical bone defect was then created in the proximal diaphysis of the anteromedial aspect of the left tibia of each rabbit by using an air-powered dental drill (Vetbase 2, Henry Schein, Melville, NY) and a crosscut fissure dental burr (size 557). Harvested neoosseous tissue was placed into the defect and secured in place by reapposition of muscle fascia separated during exposure. Closure was achieved as before. In an additional two rabbits, cortical bone defects were created bilaterally and filled with a gelatin sponge (Gelfoam, Amersham Pharmacia and Upjohn). Lateral and anteroposterior radiographs of operated legs were obtained before and after surgery and at 2-week intervals until death at 6 weeks postoperatively (Transworld 325V X-Ray Control and Generator, Transworld X-Ray, Charlotte, NC).

Characterization of Neo-Bone. ***Histological analyses and histomorphometry.*** The whole tibia was demineralized with ethylenediamine tetraacetic acid before embedding in paraffin wax. Five-micrometer-thick cross sections taken at three different locations separated by 1-mm intervals through the middle of the subperiosteal bioreactors were used for the determination of histomorphometric parameters, the terms of which are defined as outlined by the American Society for Bone and Mineral Research histomorphometry nomenclature committee (18). The sections were stained with hematoxylin/eosin (H&E) or safranin-O and the bone-bioreactor space and the surrounding area examined under a light microscope. Immunohistochemical analysis was performed by using a monoclonal antibody to detect the presence of osteonectin (ADN-1, Developmental Studies Hybridoma Bank, Iowa City, IA) and collagen type II (II II6B3, Developmental Studies Hybridoma Bank) by using a method previously described (19). Immunohistochemical analysis to detect the presence of type I collagen was performed by using a monoclonal antibody to collagen I (ab6308, Abcam, Ltd., Cambridge, U.K.). Immunostaining used an indirect avidin–biotin–peroxidase technique (ABC, Vector Laboratories) with diaminobenzidine as the chromogen for the antigen localization. Mouse IgG (Vector Laboratories) was used as a negative control. Sections through undecalcified tibia were obtained by embedding the whole tibia in methylmethacrylate (Sigma) by using a method previously described (20). Five-micrometer-thick ground cross sections taken through the middle of the subperiosteal bioreactor were stained with von Kossa and Goldner's trichrome and examined under a light microscope.

Mechanical characterization. Rectangular specimens of dimensions 4 $\times$ 1 $\times$ 2 mm were machined at low speed under continuous irrigation from neo-bone harvested from the bone bioreactor or bone harvested from the anteromedial side of the tibia (control). Because of the mechanical anisotropy of bone, specimens were

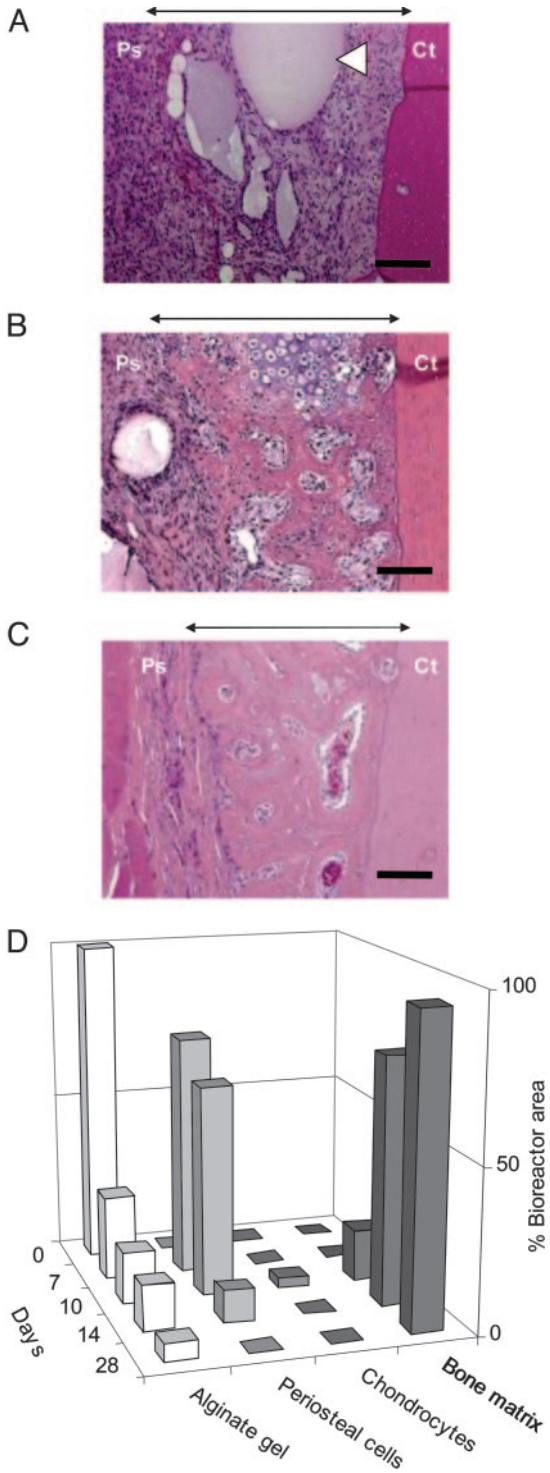

Fig. 1. Tissue evolution within the bioreactor space in a rabbit tibia, in the absence of growth factors. H&E cross sections through the bioreactor space and adjacent cortical bone of the tibia after (*A*) 7, (*B*) 10, and (*C*) 14 days. White arrowhead indicates unresorbed alginate gel. Black arrows indicate area occupied by the bioreactor. Ps, periosteum; Ct, cortical bone of the tibia. (Bar, 100 μm.) (*D*) Time course of tissue progression and gel resorption.

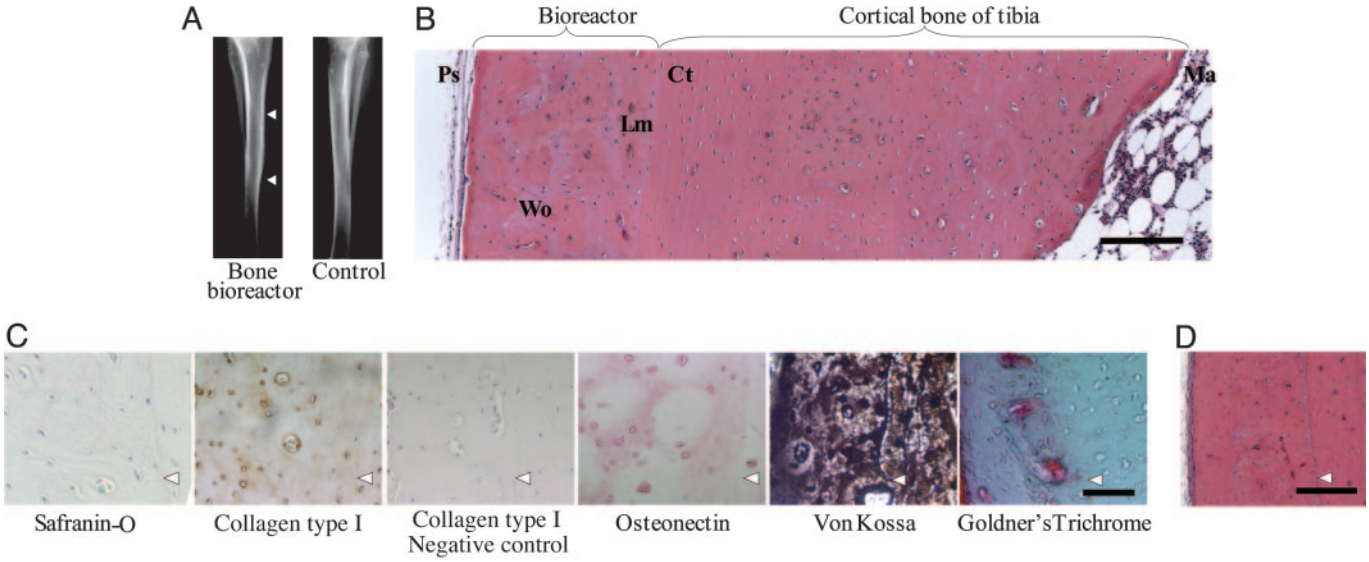

Fig. 2. Histological characterization of the tissue within the bioreactor in absence of growth factors. (*A*) Radiograph of tibia with the bioreactor (right leg) and contralateral limb after 6 weeks. Arrowheads indicate top and bottom of bioreactor. (*B*) H&E-stained cross section of the bone bioreactor, adjacent cortical bone, and marrow cavity after 6 weeks. Ps, periosteum; bone, Wo, woven; Lm, lamellar; Ct, cortical; Ma, marrow. (Bar, 300 μm.) (*C*) Immunostaining for type I collagen and osteonectin and staining for hydroxyapatite mineral phase after 6 weeks. Arrowheads indicate demarcation between bioreactor space (on the left) and cortical bone (on the right). (Bar, 50 μm.) (*D*) H&E-stained cross section of the bone bioreactor and adjacent cortical bone after 8 weeks. Arrowhead indicates demarcation between bioreactor and tibia. (Bar, 250 μm.)

oriented with their long axes parallel to the long axis of the bone (21). After machining, the specimens were kept frozen at −20°C and allowed to equilibrate in a hydrated state in PBS to room temperature (23°C) before testing (22).

Compressive testing of the bone samples was performed by using an Instron-5542 (Instron, Canton, MA) instrument with a 500 N load cell. Compressive stress, extension, and load were recorded with MERLIN MATERIALS TESTING software (Version 4.42, Instron). The machine test was set to stop at a 60% drop in load, indicating severe mechanical failure of the sample. A strain rate of 0.01 $\varepsilon.s^{-1}$ was chosen to mimic normal bone activity (23). Because of the small size of the sample specimens, machine compliance (K) was determined for all measurements and the extension data corrected accordingly.

Results and Discussion

To engineer bone, we created the bioreactor between the surface of a long bone (tibia) and the membrane rich in pluripotent cells that covers it, namely the periosteum (24). Controlled manipulation of the periosteal space was achieved by using a hydraulic elevation procedure that was recently developed in our laboratory (17). Once the space of the desired geometry was created, the space was filled with calcium-alginate gel. The procedure allowed us to create a space that reproducibly accommodated a gel 200 mm^3 in volume.

We followed the evolution of the bioreactor space over time and observed that one of the early events was the rapid proliferation of cells within the inner layer of the periosteum. Unlike a typical wound-healing response that is dominated by infiltration of fibroblasts, by day 3 the bioreactor space was filled with spindle-shaped periosteal cells and capillaries (data not shown) (25). Instead of a fibroblast-rich scar tissue, we observed woven bone at 2 weeks, which subsequently evolved into compact bone tissue at later time points. An unexpected outcome of the pinhole incision used to create the subperiosteal space via hydraulic elevation was that it had effectively eliminated other external cell populations, thus favoring the recruitment and proliferation of cells local to that environment, namely the progenitor cells from the inner cambium layer of the periosteum (26). In contrast, the creation of a subperiosteal space using a wider (2-mm) incision resulted in the formation of fibroblast-dominated scar tissue ($n = 2$, data not shown).

The choice of gel filler was based on the premise that the presence of calcium within the matrix would favor osteogenic differentiation of the appropriate progenitor cell population (24–27). The stages of neo-bone formation appeared to follow a path akin to intramembraneous bone formation, as observed in skeletal formation in a developing embryo and during fracture repair, when osteogenic cells in the presence of a good blood supply and adjacent to a local deposit of calcium salts will differentiate into bone cells (Fig. 1) (24–27). Although on a less-frequent basis, we also observed the presence of hypertrophic chondrocytes within the bioreactor space (Fig. 1 *B* and *D*). Therefore, it is equally plausible that the process of neo-bone formation occurs via an endochondral pathway, wherein the cartilage template is rapidly remodeled/resorbed to yield bone. By day 10, woven bone incorporating large (40- to 180-μm) vascular canals had formed, which progressively increased during the next 4 days [16.5 ± 3.0% (day 10) and 76.1 ± 14.0% (day 14) of the cross-sectional area of the bioreactor space] with a concurrent disappearance of the alginate-gel matrix (Fig. 1 *B* and *C* and Fig. 5, which is published as supporting information on the PNAS web site). Since the alginate is not metabolized, the most likely mechanism of resorption is through dissolution. The woven bone matrix subsequently matured into fully mineralized compact bone (Fig. 2). A neovascularization process that resolved by 12 weeks accompanied the formation of neo-bone. We have verified that the neo-bone after 6 weeks exhibits all of the histological markers [extracellular matrix components (ECM)] of native bone and structural characteristics such as osteons surrounded by concentric layers of lamellar bone (Fig. 2). Specifically, the neo-bone stained positive for osteonectin and collagen type I, which is the primary ECM component of bone, and negative for collagen type II and safranin-O, which are specific to cartilaginous tissue (Fig. 2*C*). von Kossa staining performed on undecalcified neoosseous tissue revealed that mineralization of the neo-bone had occurred, and that the mineral phase was hydroxyapatite (stained green with Goldner's

Table 1. Histomorphometrical analysis of bone formation in bioreactors

Time point, weeks	Growth factor	Alginate, %	Vascular canals, %	Tissue, matrix %	Bone, tissue %
6	None	0.18 ± 0.25	7.44 ± 6.56	92.39 ± 6.80	99.82 ± 0.25
6	T/F	2.91 ± 2.85	17.81 ± 8.36	79.29 ± 10.79	97.10 ± 2.85
8	None	1.10 ± 1.56	18.55 ± 9.12	80.35 ± 10.68	98.90 ± 1.56
8	T/F	0.73 ± 0.84	14.06 ± 12.19	85.21 ± 11.91	99.28 ± 0.84
12	None	0.28 ± 0.40	7.83 ± 4.49	91.89 ± 4.09	99.71 ± 0.40
12	T/F	0.96 ± 1.23	6.00 ± 7.13	93.04 ± 8.36	99.04 ± 1.23

n = six bioreactors per time point, three of which contained TGF-β1 and FGF-2. Parameters were measured in cross sections through the middle of the bioreactor space (n = 3) for each bioreactor. Data are expressed as mean ± standard deviation. T/F indicates the inclusion of TGF-β1 and FGF-2 in the formulation.

trichrome) (Fig. 2*C*). After 8 weeks, a further maturation of the osseous tissue is observed with a concurrent decrease in the proportion of woven bone and increase in lamellar bone sheets (Fig. 2*D*). The high population of vascular canals observed at 6 and 8 weeks (angiogenesis associated with the process of osteogenesis) decreased after a period of 12 weeks to a level comparable to the population of vascular canals of mature compact bone (Table 1). The maximum thickness of neo-bone obtained in this study was 1.5 mm (Fig. 6, which is published as supporting information on the PNAS web site), and it corresponded to a volume of ≈162 mm^3. Interestingly, we observed that if the pocket was filled with a viscous alginate solution that was not crosslinked with calcium ions, the volume of neo-bone regenerated was 10-fold less after 6 weeks and typically ≈15 mm^3. This observation underscores the choice of a calcium-rich gel, as hypothesized earlier. The volume of bone engineered in a rabbit is sufficient for a single interbody fusion procedure in the same animal. This is based on the following analysis: Typically 4–6 cc of cancellous bone is required for a single interbody fusion procedure in a human. When scaled down to a rabbit mass (weight: human ≈70 kg, rabbit ≈2 kg), one would require ≈0.17 cc (170 mm^3) of cancellous bone. An important outcome of the procedure used in this study was the reproducibility of the volume of neo-bone formed (162 ± 6 mm^3 for a procedure tested >25 times). Upon reducing the bioreactor dimensions to 1-cm long, 0.7-cm wide, and 1-mm thick, the final volume of the neo-bone was 3-fold less (55 mm^3), suggesting an extremely close correlation between pocket size and volume of bone. This suggests that neomorphogenesis events within the bioreactor space are confined to and dictated by the biomaterial volume. For both bioreactor sizes, however, the volume of bone generated was 20% less than the volume of gel injected. This reduction in volume can be attributed to a possible compression of the bioreactor space by the periosteum and/or contractile forces exerted on the biomaterial by mesenchymal cells. The biomaterials role in dictating neo-bone volume was confirmed by the observation that if the pocket was left unfilled, no new bone formation was observed even after 6 weeks (n = 4).

We determined the mechanical properties of the neo-bone and found that its compressive strength [Young's modulus of 17.4 ± 3.9 GPa (n = 5)] was within the range that is typical of compact bone (15–29 GPa) (28). The mean values of 115.2 ± 17.1 MPa (n = 5) for the ultimate strength of the neo-bone specimens also fall within the range for compact bone (100–300 MPa, human: 193 MPa) (28) (see Fig. 7 and *Supporting Text*, which are published as supporting information on the PNAS web site). These results suggest that the mineral phase, which is composed of hydroxyapatite and responsible for the stiffness of bone, is distributed and present in quantities that are at the least comparable to native bone. Importantly, structural characteristics such as osteons are also arranged along the load axis as in native load-bearing bone.

An extremely significant outcome of the "*in vivo* bioreactor" approach is that the events accompanying neo-bone formation are achieved without local or systemic administration of growth factors, other biomolecules or cell isolation and transplantation. Nevertheless, we investigated whether localized coadministration of exogenous FGF-2 and TGF-β1, which are known to promote chondrogenesis in periosteal explants *ex vivo* (13),

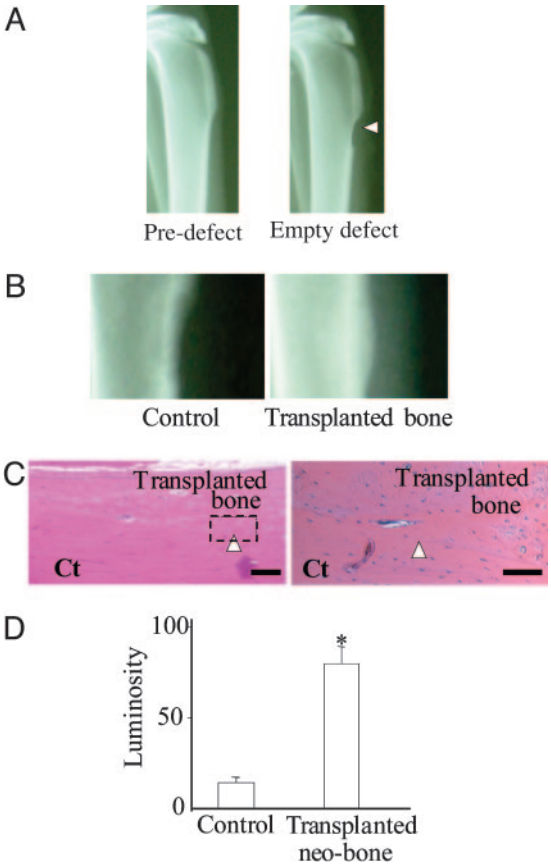

Fig. 3. Autologous bone transplantation. (*A*) Radiography of typical rabbit tibia before and after creation of cortical bone defect. Arrowhead indicates empty defect. (*B*) Magnified radiographs of rabbit tibia defects 6 weeks after transplantation of Gelfoam (control) and autologous bone from the bone bioreactor in the contralateral tibia. (*C*) H&E-stained sections of the defect site 6 weeks after transplantation of autologous bone. Arrowhead points to the integration between transplanted bone and cortical bone of the tibia. Ct, cortical bone. [Bars, (*Left*) 200 μm; (*Right*) 50 μm.] (*D*) Radiographic densitometry evaluation of the tibial defects in grafted (n = 4) and control group rabbits (n = 4) after 6 weeks. (*, $P < 0.1$, ANOVA), presented as standardized luminosity where an empty defect has a value of 0, and cortical bone has a value of 100.

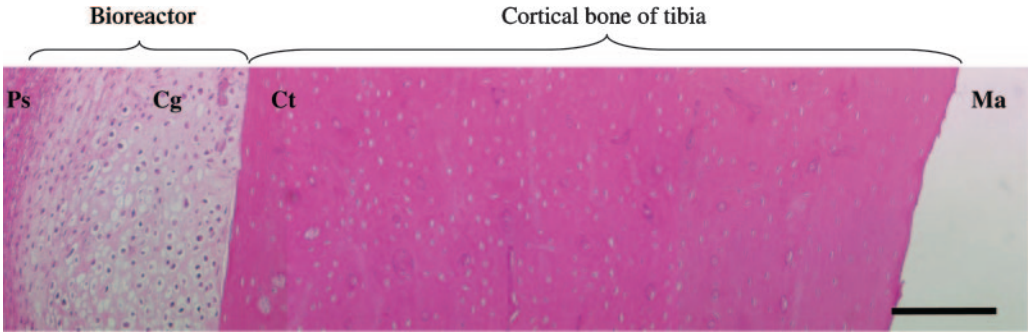

Fig. 4. H&E-stained cross section of cartilage in the bioreactor and adjacent cortical bone 10 days after HA gel containing Suramin was introduced into the bioreactor. Ps, periosteum; Cg, cartilage; Ct, cortical bone of the tibia; Ma, marrow space. (Bar, 300 μm.)

would enhance bone formation by promoting ossification via an endochondral route. Although we observed a general trend of increased neo-bone formation and vascularity at earlier time points (6 weeks), the difference in bone volume was not statistically significant ($P > 0.1$, Table 1). This observation serves to strengthen the premise that with this tissue regeneration approach, the inductive cues are derived locally i.e., *in vivo*, the localized secretion of endogenous mitogens and morphogens as a part of the wound healing response, and the presence of vasculature (29–31) may be leveraged for the controlled *de novo* formation of vascularized tissues such as bone. Growth factor administration, possibly through controlled release formulations (32), however, may aid the formation of neo-bone in instances of age or disease-related reduction in periosteum viability, through a variety of mechanisms including increased angiogenesis and proliferation of the periosteal cells (Table 1) (33–36).

We believe that the *in vivo* bone regeneration approach presented herein is particularly relevant for spinal fusion applications, where quality of bone has a tremendous impact on clinical outcomes. In spinal fusion, autologous bone is considered the gold standard because of its ability to integrate with the host bone and lack of immune-related complications (3). Nevertheless, the use of autologous bone has been hampered because of the pain and long-term discomfort that accompany such harvests from the iliac crest (4). The importance of donor site morbidity was underscored in a recent study that showed the overall midterm results of a single-level interbody fusion at the cervical spine were impaired more by the iliac crest harvest than by the spinal fusion procedure itself, and that >26% of patients reported chronic pain at the donor site as late as 2–6 years postoperatively (4). The approach presented herein would allow for the generation of large quantities of autologous bone not only on demand but also at a site that is surgically easily accessed with few associated complications, namely the epiphyseal region of long bones.

We carried out autologous transplantation studies with the aim of addressing the following questions: (*i*) Can the engineered bone be harvested? (*ii*) Will the harvested bone integrate at a recipient site? To study this, a C-shaped defect in the cortical bone of the tibia of the contralateral leg was used as a model recipient site. With respect to neo-bone harvest, we found that the demarcation between the neo-bone and the cortical bone of the tibia acted as a point of weakness that enabled the neo-bone to be harvested while leaving the underlying normal skeletal architecture uncompromised (Fig. 8, which is published as supporting information on the PNAS web site). Radiographical and histological assessment of the fate of the neo-bone at the transplant site after a period of 6 weeks revealed that the engineered bone had remodeled and integrated with the surrounding bone in the defect (Fig. 3). This observation is consistent with several studies (37) that have shown that when the bone is fresh and vascularized, graft uptake and integration are excellent even in large diseased bone sites. In contrast, when the defect site was filled with Gelfoam, a collagen scaffold known to promote bone formation when mixed with marrow elements or *rh*BMP-2, no bone formation was observed within the defect (38).

We have also explored the *in vivo* engineering of cartilage with this approach. Recent studies have shown that the controlled coadministration of Suramin and TGF-β1 from liposome formulations is highly efficacious in inhibiting vascular invasion and bone formation within the cartilaginous compartments of full-thickness articular cartilage defects that would otherwise ossify (16). In our preliminary studies, we induced hypoxia in the bioreactor environment by local administration of the antiangiogenic factor Suramin in a HA-based gel matrix. Since Suramin is known to exert a potent inhibitory effect on the TGF-β super family of proteins (39, 40), we supplemented the formulation with a small amount of TGF-β1 (20 ng per pocket) to compensate for the loss of endogenous TGF-β1. This dose of TGF-β1 in a HA gel when injected in the bioreactor in the absence of Suramin (n = two bioreactors) was not capable of inducing chondrogenesis (data not shown). In contrast, we found that the controlled delivery of liposome-encapsulated Suramin within the HA led to cartilage formation within the bioreactor after 10 days (n = two bioreactors) (Fig. 4). Although a complete quantitative analysis of chondrogenesis with the "*in vivo* bioreactor" is essential before any broad conclusions may be drawn, the results nevertheless suggest the "*in vivo* bioreactor" environment is conducive to cartilage regeneration and may lend itself to the *in vivo* engineering of osteochondral composites. *In vivo* engineering of hyaline cartilage would have important implications for joint resurfacing and reconstruction, particularly if, as shown here, the cartilage can be associated with a phase such as bone or periosteum that is capable of integration with articular subchondral bone (41, 42).

The potential for using the *in vivo* bone bioreactor in humans as a means of engineering autologous bone for banking and transplantation is bolstered by our preliminary findings that a confined subperiosteal space can be created in human tibiae with an elevation of 1 cm between the mesenchymal cambium layer and the underlying bone (see Fig. 9, which is published as supporting information on the PNAS web site). Because the *in vivo* tissue-engineering approach described enables controlled cellular proliferation, differentiation, and hierarchical organization within an artificial cavity in the body, it may be useful also in the *de novo* synthesis of other highly vascularized and multicellular organs such as liver.

This paper is dedicated to the memory of Dirk Schaefer. We thank Ivan Martin, Ernst Hunziker, and Marsha Moses for their insightful comments. The HA gel was a kind gift from X. Jia (Massachusetts Institute of Technology, Cambridge, MA). This work was supported by a grant from Smith and Nephew, Endoscopy.

1. Einhorn, T. A. (1995) *J. Bone Joint Surg. Am.* **77,** 940–956.
2. Boden, S. D. (2002) *Spine* **27,** S26–S31.
3. Bauer, T. W. & Muschler, G. F. (2000) *Clin. Orthop. Relat. Res.* **371,** 10–27.
4. Silber, J. S., Anderson, D. G., Daffner S. D., Brislin, B. T., Leland, J. M., Hilibrand, A. S., Vaccaro, A. R. & Albert, T. J. (2003) *Spine* **28,** 134–139.
5. Breitbart, A. S., Staffenberg, D. A., Thorne, C. H., Glat, P. M., Cunningham, N. S., Reddi, A. H., Ricci, J. & Steiner, G. (1995) *Plast. Reconstr. Surg.* **96,** 699–708.
6. Paul, W. & Sharma, C. P. (2003) *J. Biomater. Appl.* **17,** 253–264.
7. Petite, H., Viateau, V., Bernsaid, W., Meunier, A., De Pollak, C., Bourguignon, M., Oudina, K., Sedel, L. & Guillemin, G. (2000) *Nat. Biotechnol.* **18,** 959–963.
8. Warnke, P. H., Springer, I. N. G., Wiltfang, J., Acil, Y., Eufinger, H., Wehmoller, M., Russo, P. A. J., Bolte, H., Sherry, E., Behrens, E., *et al*. (2004) *Lancet* **364,** 766–770.
9. Thomson, R. C., Mikos Antonios, G., Beahm, E., Lemon, J. C., Satterfield, W. C., Aufdemorte, T. B. & Miller, M. J. (1999) *Biomaterials* **20,** 2007–2018.
10. Simmons, C. A., Alsberg, E., Hsiong, S., Kim, W. J. & Mooney, D. J. (2004) *Bone* **35,** 562–569.
11. Rose, F., R., Hou, Q. & Oreffo, R. O. (2004) *J. Pharm. Pharmacol.* **56,** 415–427.
12. Stevens, M. M., Qanadilo, H. F., Langer, R. & Shastri, V. P. (2004) *Biomaterials* **25,** 887–894.
13. Stevens, M. M., Marini, R. P., Martin, I., Langer, R. & Shastri, V. P. (2004) *J. Orthopaed. Res.* **22,** 1114–1119.
14. Bulpitt, P. & Aeschlimann, D. (1999) *J. Biomed. Mater. Res.* **47,** 152–169.
15. Kim, S., Turker, M. S., Chi, E. Y., Sela, S. & Martin, G. M. (1983) *Biochim. Biophys. Acta* **728,** 339–348.
16. Hunziker, E. B. & Driesang, I. M. K. (2003) *Osteoarthr. Cartilage* **11,** 320–327.
17. Marini, R. P., Stevens, M. M., Langer, R. & Shastri, V. P. (2004) *J. Invest. Surg.* **17,** 229–233.
18. Parfitt, A. M., Drezner, M. K., Glorieux, F. H., Kanis, J. A., Malluche, H., Meunier, P. J., Ott, S. M. & Recker, R. R. (1987) *J. Bone Miner. Res.* **2,** 595–610.
19. Schaefer, D., Martin, I., Shastri, P., Padera, R. F., Langer, R., Freed, L. E. & Vunjak-Novakovic, G. (2000) *Biomaterials* **21,** 2599–2606.
20. Emmanual, J., Hornbeck, C. & Bloebaum, R. D. (1987) *Stain Technol.* **62,** 401–410.
21. Currey, J. D. (2002) *Bones: Structure and Mechanics* (Princeton Univ. Press, Princeton).
22. Sedlin, E. D. & Hirsch, C. (1966) *Acta Orth. Scand.* **37,** 29–48.
23. Cowin, S. C. (2001) *Bone Mechanics Handbook* (CRC Press, Boca Raton, FL), 2nd Ed.
24. Jacobsen, F. S. (1997) *J. Pediatr. Orthrop. B* **6,** 84–90.
25. Ham, A. W. (1930) *J. Bone Joint Surg.* 827–844.
26. Aoki, J., Yamamoto, I., Hino, M., Kitamura, N., Sone, T., Itoh, H. & Torizuka, K. (1987) *Skeletal Radiol.* **16,** 545–551.
27. Chanavaz, M. (1995) *J. Oral Implant.* **21,** 214–219.
28. Erickson Gregory, M., Catanese, J., 3rd, & Keaveny Tony, M. (2002) *Anat. Rec.* **268,** 115–124.
29. Assoian, R. K. & Sporn, M. B. (1986) *J. Cell Biol.* **102,** 1217–1223.
30. Hill, D. J. & Logan, A. (1992) *Prog. Growth Factor Res.* **4,** 45–68.
31. Probst, A. & Spiegel, H. U. (1997) *J. Invest. Surg.* **10,** 77–86.
32. Langer, R. (1992) *Experientia* **61, S**327–S330.
33. De Bari, C., Dell'Accio, F. & Luyten, F. P. (2001) *Arthritis Rheum.* **44,** 85–95.
34. Joyce, M. E., Terek, R. M., Jingushi, S. & Bolander, M. E. (1990) *Ann. N. Y. Acad. Sci.* **593,** 107–123.
35. Joyce, M. E., Roberts, A. B., Sporn, M. B. & Bolander, M. E. (1990) *J. Cell Biol.* **110,** 2195–2207.
36. Joyce, M. E., Jingushi, S. & Bolander, M. E. (1990) *Orthrop. Clin. North Am.* **21,** 199–209.
37. Habal, M. B. & Reddi, A. H., eds (1992) in *Bone Grafts and Bone Substitutes* (Saunders, Philadelphia), pp. 20–21.
38. Finn, M. D., Schow, S. R. & Schneiderman, E. D. (1992) *J. Oral Maxil. Surg.* **50,** 608–612.
39. Meyers, M. O., Gagliardi, A. R., Flattmann, G. J., Su, J. L., Wang, Y.-Z. & Woltering, E. A. (2000) *J. Surg. Res.* **91,** 130–134.
40. Coomber, B. L. (1995) *J. Cell. Biochem.* **58,** 199–207.
41. Buckwalter, J. A. (2002) *Clin. Orthrop. Relat. Res.*, 21–37.
42. Gross Allan, E. (2003) *J. Arthroplasty* **18,** 14–17.